Chinese Journal of Aeronautics 25 (2012) 871-878

Contents lists available at ScienceDirect

Chinese Journal of Aeronautics

journal homepage: www.elsevier.com/locate/cja

Unsteady Flow Variability Driven by Rotor-stator Interaction at Rotor Exit

ZHAO Ben[a], YANG Ce [a,*], CHEN Shan [a], QI Mingxu [a], ZHOU Mi[b]

[a]*School of Mechanical and Vehicular Engineering, Beijing Institute of Technology, Beijing 100081, China*

[b]*Basic Subject Department, Bohai Shipbuilding Vocational College, Huludao 125000, China*

Received 2 September 2011; revised 20 December 2011; accepted 1 April 2012

Abstract

Numerical investigation of the unsteady flow variability driven by rotor-stator interaction in a transonic axial compressor is performed. Two models with close and far axial gap between rotor and stator rows are studied in the simulation. Particular attention is attached to the analysis of mechanisms involved in driving rotor wake oscillation, rotor wake skewing and flow angle fluctuation at rotor exit. The results show that smaller axial gap is favorable to enhance the interaction in the region between two adjacent rows, and the fluctuation of the static pressure difference between two sides of rotor wake is improved by potential field from down stator, which is the driving force for rotor wake oscillation. The interaction between rotor and stator is weakened by increasing axial distance, rotor wake shifts to suction side of rotor blade with 5%-10% of rotor pitch, the absolute value of flow angle at rotor exit is less than that in the case of close interspace for every time step, and the fluctuation amplitude is also decreased.

Keywords: transonic compressor; numerical simulation; rotor-stator interaction; unsteady flow; wake oscillation

1. Introduction

The axial compressor has been widely used in aircraft engine and gas turbine, and it plays an important role in modern industry. The flow in turbomachines is highly unsteady and turbulent because of the aerodynamic interaction between the adjacent rows due to the effect of wakes and potential flow field. The blade/vane wake oscillation is a typical unsteady flow, which can lead to variability in interaction noises, mixing between wake and main flow and inlet Mach number to downstream impeller. In addition, the downstream blade boundary layer development can also be changed largely by the incoming wake oscillation, and then compressor performance may be influenced. Therefore, it is very important to include this phenomenon into design process to further improve the performance.

Several researchers have been conducted to investigate wake oscillation phenomenon, which indicate that it was associated with the upstream blade wake and potential field of the downstream impeller. Oro, et al. [1] used hot-wire anemometry to obtain the phase averaged velocity and found out that the velocity deficit in wake region was modified and its position changed over time. Key, et al. [2] studied rotor wake variability in a multistage compressor. Time-resolved flow angle data were acquired with a cross-film sensor. At downstream rotor exit, ensemble-averaged revolutions of data showed an amplitude modulation caused by interactions with the rotor wakes from upstream blade rows. Strazisar [3] used laser anemometry to study a transonic fan rotor. The wakes oscillated with amplitude of

*Corresponding author. Tel.: +86-10-68911373.
E-mail address: yangce@bit.edu.cn

Foundation items: National Natural Science Foundation of China (51176013); Ph.D. Programs Foundation of Ministry of Education of China (20091101110014); National High-tech Research and Development Program of China (2007AA050502)

doi: 10.1016/S1000-9361(11)60457-3

4%-6% of the pitch. Albert and Fleeter [4] investigated multistage interaction effects on rotor blade-to-blade wake variability. Multistage interactions significantly affect the rotor wake characteristics and lead to the possible generation of rogue wakes.

Up to now, the rotor-stator interaction is still a hot topic in the field of turbomachines. Mailach and Vogeler [5] tested an axial compressor with inlet guide vane (IGV) and focused on downstream stator's boundary unsteady flow. The results indicated that the unsteady boundary layer development was influenced strongly by incoming wakes. Estevadeordal, et al. [6] performed PIV study of wake-rotor interactions in a transonic compressor at various operating conditions. He concluded that vortex shedding from the wake generator and the passage of the rotor-bow shock were strongly synchronized. The rotor-stator interaction phenomenon was also described in the investigations of Refs. [7]-[10].

The unsteady flow in the region between rotor and stator blade rows is highly influenced by axial distance, which must be related to the performance of the compressor. Gorrell, et al. [11] carried out investigation of wake-shock interactions in a transonic compressor with digital particle image velocimetry and showed the time-accurate computational fluid dynamics (CFD). His research showed that the interaction strength between wake and downstream blade was enhanced by decreasing the blade-row interspace, which had an effect on the compressor performance. Li, et al. [12] studied the influence of rotor-stator spacing on the loss in one-stage transonic compressor, and indicated that smaller axial gap was favorable in reducing the irreversibility in the compressor. The effects of axial gaps on clocking effects were investigated by Ref. [13]. Their results showed that the efficiency was improved by reducing the distance between two stators in axial direction.

By summing up the open literature, we can find out that: a) stator wake oscillation is associated with potential field of downstream rotor; b) the axial interspace plays an important role in the unsteady flow in the field between rotor and stator rows. However, no research exposes whether the weak potential field of downstream stator is enough to drive the upstream rotor wake oscillation and how the driving force is influenced by axial distance.

Therefore, this paper presents numerical investigations of unsteady aerodynamic blade row interactions with axial distance varied in a transonic compressor. Different potential field strengths can be modulated by changing blade-row gap. By comparing the flow field for two models with different axial interspace, we can find out the physical mechanism of driving rotor wake oscillation which leads to flow angle fluctuation variability at rotor exit, and finally the relationship between rotor wake oscillation and axial distance between rotor and stator rows is concluded.

2. Numerical Methods and Comparison of Experimental and Calculated Results

In 1978, Reid and Moor designed and tested four compressor stages and NASA Stages 35-38 to investigate the effects of blade camber and aspect ratio on compressor performance [14]. Stage 35 and Stage 37 had the best performance. These blade rows have since been used for several CFD code assessment projects, and Stage 35 was chosen for the present work. Stage 35 is an inlet stage for a core compressor. It has 36 multiple circular-arc rotor blades and 46 circular-arc stator blades, with a design pressure ratio of 1.865 for the rotor and 1.82 for the stage at a mass flow of 20.188 kg/s. Detailed information on the geometry and experiment of the Stage 35 can be found in Ref. [15].

In order to complete the comparison of rotor wake oscillation for different blade-row interspace and in consideration of small axial distance between rotor and stator, this paper selects Stage 35 as close interspace model. Shift the stator row along the axial direction to downstream for 10 mm as far interspace model. Figure 1 shows the schematic diagram of blade-row interspace.

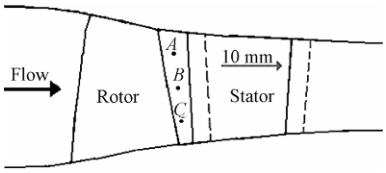

Fig. 1 Schematic diagram of blade-row interspace.

For the computation, the commercial software FINE/TURBO was utilized. The computational grid was generated using the IGG/Autogrid software package. Fluid field was plotted out and meshed in structured mesh, and the mesh type around the blade was O-type block.

The FINE/TURBO software solved the three-dimensional Reynolds-averaged Navier-Stokes equations in rotating and/or stationary frames of reference. In the present study, the Spalart-Allmaras model was used. The system of governing equations was advanced in time using an explicit four-stage Runge-Kutta scheme.

Residual smoothing, local time-stepping and multigrid method were employed to speed-up convergence to the solution.

The unsteady simulation was carried out at design point, and the stator was approximated as having 48 blades instead of 46 in the actual configuration. A dual time stepping method was used to perform time accurate calculations. The angle corresponding to every rotor passage is 10°, the angle of one time step is 1°, and hence every rotor passage is simulated with 10 time steps. Three rotor passages and four stator passages for computation require 30 time steps. The total

number of grid points for unsteady computation is about 3 241 833. Uniform total pressure and temperature with axial flow direction was imposed at the inlet boundary and mass flow rate was set at the outlet boundary condition for unsteady simulation. Steady computational result was selected as the initial condition for unsteady simulation.

In Fig. 2, numerical and experimental results of the compressor efficiency vs mass flow rate at 17 188.7 r/min are compared and they show acceptable agreement. In Fig. 3, the calculated pressure ratio vs mass flow rate at 17 188.7 r/min is compared with experimental results. They show that the maximum differences between numerical and experimental results for 17 188.7 r/min locate at the choke and surge area. In addition, the experiment shows lower efficiency in Fig. 2 and higher pressure ratio in Fig. 3; the maximum differences between numerical and experimental data are 1.0% and 2.0% respectively. Totally the discrepancy is in the acceptable range and the numerical model is reliable to predict and analyze this combined compressor.

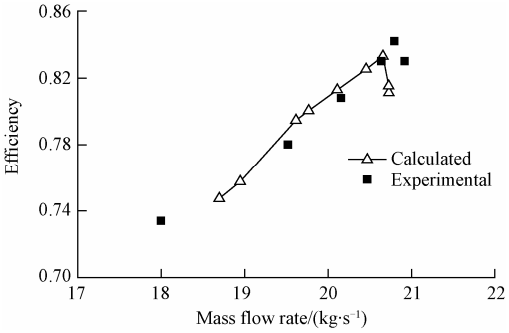

Fig. 2 Numerical and experimental results of compressor efficiency vs mass flow rate at 17 188.7 r/min.

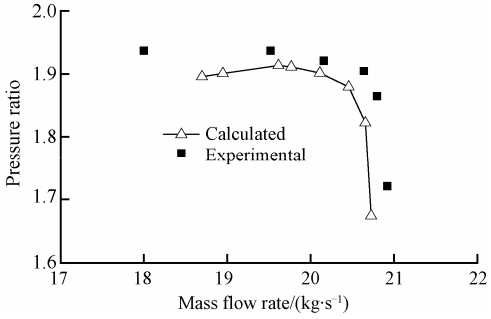

Fig. 3 Numerical and experimental results of compressor pressure ratio vs mass flow rate at 17 188.7 r/min.

3. Results and Discussion

3.1. Rotor wake oscillation

When the upstream rotor wakes passed the leading edge of stator, the wake character variability was driven by interaction with the potential field of downstream vane row. For example, Fig. 4 compares the temporal evolution of the dimensionless velocity at different spans for close interspace model (locations marked with *A*, *B* and *C* in Fig. 1). The abscissa of the graph is rotor pitch (in the rotor reference frame) and the vertical axis is dimensionless axial velocity (V_z/V), which is the instantaneous velocity V_z non-dimensionalized by overall mean velocity V. Each line in the plots corresponds to the trace of the variable every t/T=1/30 (t is the time and T represents four rotor blades passing time). These evolutions describe the flow structures of the wakes. Not only the deficit of velocity but also wake's positions change over time.

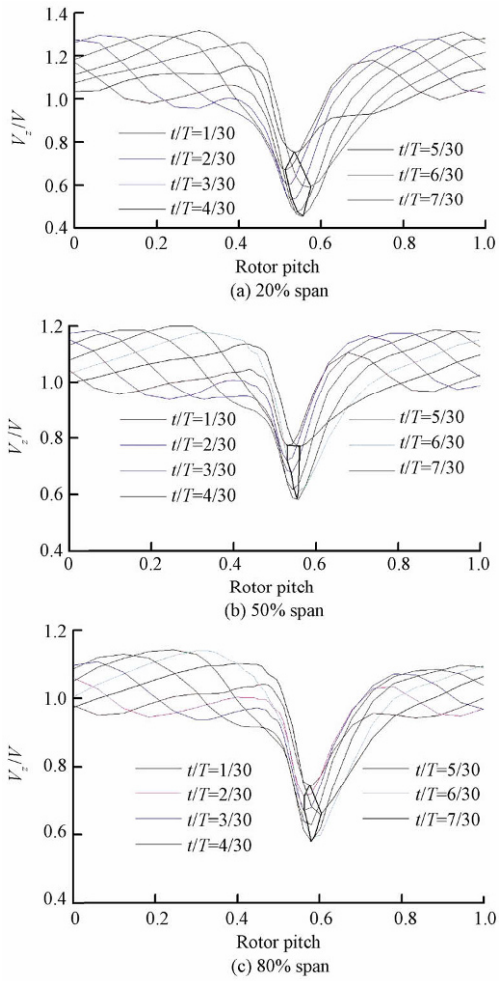

Fig. 4 Temporal evolution of dimensionless velocity at different spans for close interspace model.

Similar graphs for far interspace model are shown in Fig. 5. The rotor wake's position nearly does not change over time, and the deficit of velocity is still modified, but the ranges of velocity deficit variability are far smaller than that for close interspace model, respectively. Thus, the rotor wake oscillation characteristic and velocity deficit variability depend on axial gap between rotor and stator rows. Different axial gaps between two adjacent blade rows are also devoted to compare and analyze the response of downstream blade rows (e.g., Ref. [16]) and the improved performance (e.g., Ref. [17]).

Note that the wake oscillation is the main source of

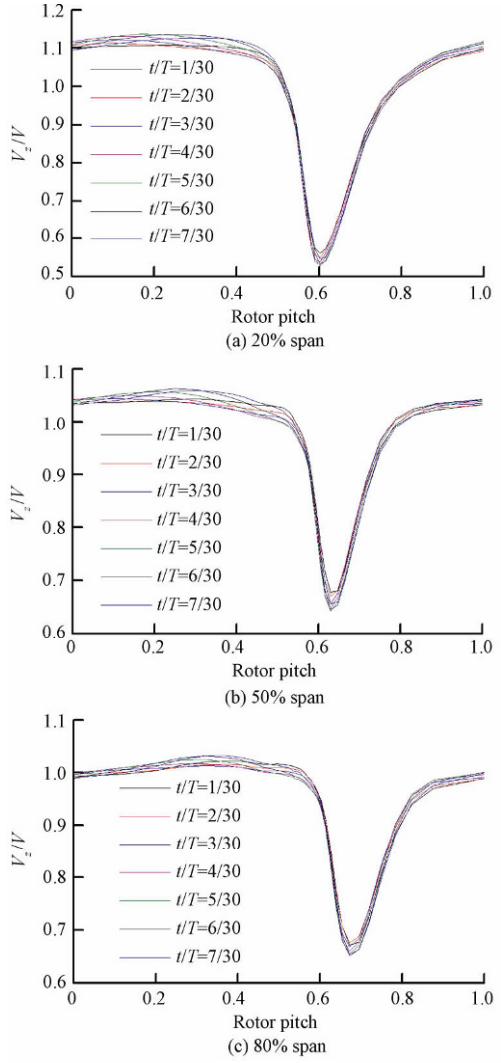

Fig. 5 Temporal evolution of dimensionless velocity at different spans for far interspace model.

the flow unsteadiness in compressors and can lead to variability in mixing between wake and free flow. The flow instability and receptivity theory must be included to explain the wake oscillation phenomenon, which is very important to include this phenomenon into design process to further improve the performance of compressor.

The entropy time-space plots at rotor exit (their positions marked with *A*, *B* and *C* in Fig. 1) at different spans for two cases of axial distance models are shown in Fig. 6 to investigate the period of rotor wake oscillation. The vertical axis shows time, non-dimensionalized by the three rotor blades' passing time, while the horizontal axis corresponds to the rotor pitch (In the rotor reference frame, we plotted three times for clarity, the close interspace model in left-hand plots and the far interspace model in right-hand plots). Vertical bands of high entropy correspond to the rotor wakes, their positions are not fixed at a particular tangential position and the wakes oscillate about their mean position with the amplitude of 5% of rotor pitch in the left plots; in contrast, they nearly keep at the same pitch positions in the right plots. As a consequence, it is supposed that the rotor wake has a cyclical oscillation for close interspace and the amplitude is concerned with downstream stator. Similarly rogue wake in multistage compressor has been investigated by Zhao, et al. [18]. Because of the value of rotor pitch changes along the span, we have a difficulty to compare the oscillation amplitudes for three spanwise locations in Figs. 5-6.

Note the flow angle variability in wake field is a significant value for comparing rotor wake oscillation strength. This paper defines a new parameter to compare the wake oscillation strength and find out the relationship between the amplitude of wake oscillation and the spanwise direction, which is called wake oscillation coefficient OC and calculated as follows.

Average flow angle is

$$\overline{\beta} = \frac{1}{N}\sum_{t/T=1/30}^{N/30}\beta(t/T) \tag{1}$$

Wake oscillation coefficient is

$$\mathrm{OC} = \sqrt{\frac{1}{N}\sum_{t/T=1/30}^{N/30}\left(1-\frac{\beta(t/T)}{\overline{\beta}}\right)^2}\times 100 \tag{2}$$

where β represents the flow angle.

Figure 7 compares the OC value for three spanwise positions at rotor exit. Because the flow is complex, highly unsteady in wake field, the OC value is greater in wake than that at rotor passage exit. The positive peak location corresponds to rotor wake field. Significant differences are also observed in the rotor wake field in Fig. 7. The peak-value at 20% span is the largest among three curves in Fig. 7, while it is the smallest at 80% span, because the axial distance increases along the spanwise direction (see Fig. 1). Moreover, the OC value for the curve is much larger in Fig. 7(a) than that in Fig. 7(b) at the same spanwise position, respectively. We can also explain the phenomenon with varied axial interspace between rotor and stator rows. Therefore, the amplitude of the wake oscillation at 20% span is the largest among three spanwise positions for each model.

3.2. Physics mechanism of driving wake oscillation

The rotor wakes oscillate over time as the impeller located at close axial distance, while, the phenomenon disappears when the axial distance between the upstream rotor and downstream stator rows is increased by 10 mm. Moreover, the axial distance, which increases between two adjacent impellers, decreases the OC value alone the radial direction. It is well known that the rotor wakes are chopped by the stator leading edge, producing new unsteady phenomena, which modifies the wake pattern and contributes to rotor wake oscillation and deficit of velocity.

Figure 8 shows the sketch of stator-rotor interaction for two axial distance models at 20% span (Note the OC peak-value is the maximum at 20% span for Fig. 7, the close interspace model in Fig. 8(a) and the far in-

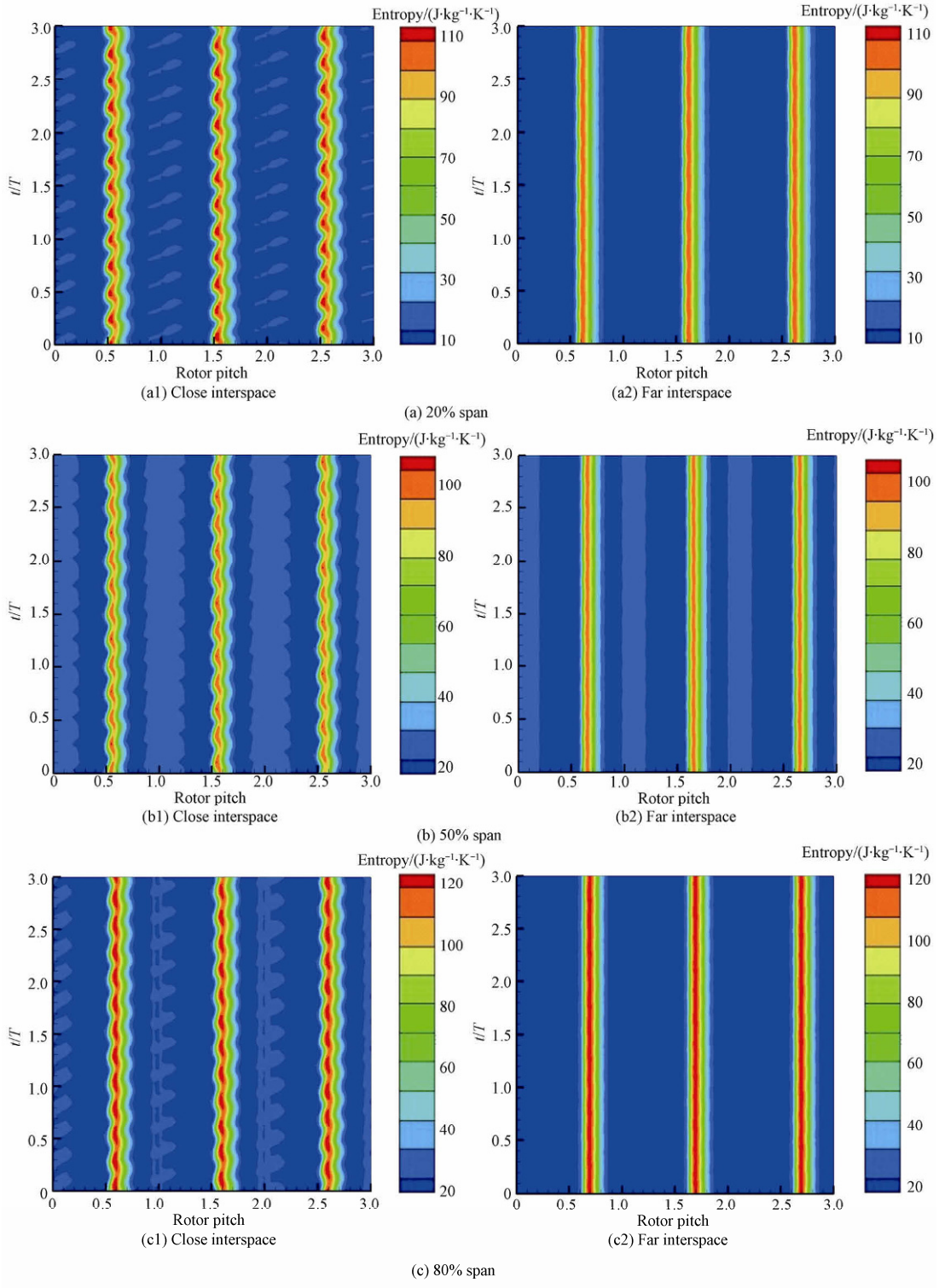

Fig. 6 Comparison of entropy variation at rotor exit between close interspace and far interspace.

terspace model for Fig. 8(b)). For that purpose, normalized axial velocity component is plotted over time at rotor exit for both the close interspace and the far interspace models. The straight lines crossing the plots diagonally represent the downstream stator leading edge positions. The value of dimensionless axial velocity in the field interacted by downstream stator leading edge is reduced obviously. As the rotor wake faces the vane leading edge, the velocity deficit is enhanced especially because of the geometrical blockage of vanes, which reduces the wake velocity magnitude as a result. In addition, due to the flow acceleration when the rotor wake enters in the stator passage, the deficit is reduced; but we have a difficulty to find out the similar phenomenon in Fig. 8(b). As is evident, the axial velocity component is influenced by geometry blockage, which is also associated with blade-row interspace. On the other hand, the rotor wake's position changes over time

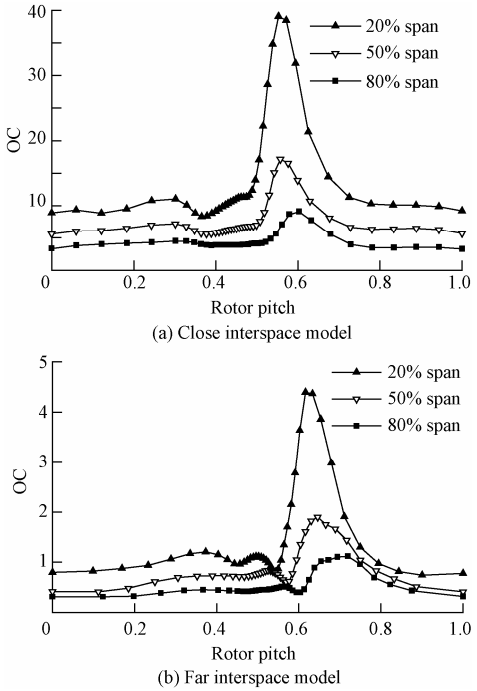

Fig. 7 OC value distribution for three spanwise positions at rotor exit.

steps in Fig. 8(a). The rotor wake's position locates at 0.5 rotor pitch in Fig. 8(a) at t/T=1/30, while it shifts towards the suction side of blade at the time range from t/T=1/30-5/30. At t/T=5/30, the rotor wake's position is located at 0.55 rotor pitch in Fig. 8(a). At the next time step, it shifts towards the pressure side of blade. No similar phenomenon is found in Fig. 8(b). Also, these results show that rotor wake oscillation is associated with the interaction between vane and rotor wake. These conclusions are similar to those found in Fig. 6.

Further insight into the rotor wake oscillation driven by the interaction between rotor wake and stator is completed through analyzing the influence by potential field. Figure 9 represents distribution of static pressure at 50% span for the case with smaller interspace model and is also employed to provide insight of the potential mechanisms acting on the rotor wake. The blades have been marked with red color, the curves are the static pressure isolines, and the high pressure and low pressure fields are marked respectively with words in Fig. 9. The negative and positive tangential pressure gradients can be found in one rotor pitch (The contour lines represent tangential pressure gradient directions, "+" stands for high pressure field and "−" low pressure field). In the region marked with N, the negative pressure gradient induces the rotor wake flow to overturn towards the suction side of blade, and it corresponds to the time range from t/T=1/30-5/30 in Fig. 8(a). In contrast, in another region marked with P, the positive pressure gradient induces the rotor wake flow to shift towards the pressure side of blade, and it corresponds to the time rang from t/T=5/30-7/30 in Fig. 8(a).

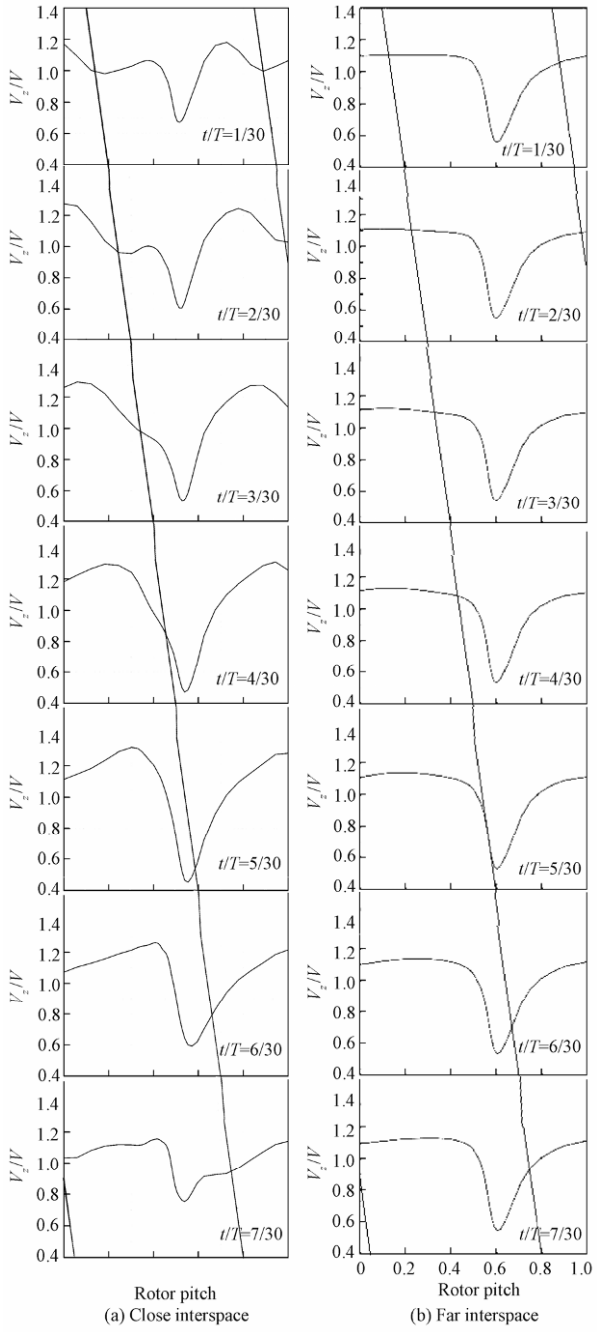

Fig. 8 Sketch of stator-rotor interaction.

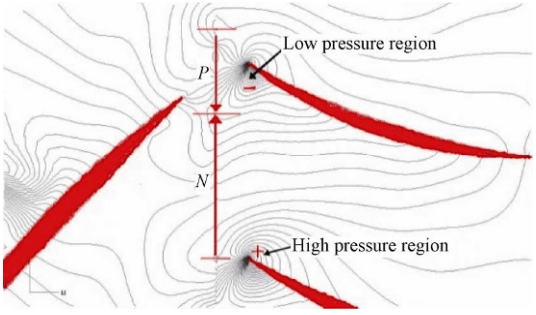

Fig. 9 Distribution of static pressure at 50% span for close interspace model, t/T = 8/30.

3.3. Rotor wake skewing

The rotor wake's positions are different for different axial distance models. The rotor wake position locates in the range of 0.5-0.55 rotor pitch for the case of smaller axial distance model, while, it locates at 0.6 rotor pitch for larger interspace models (see Fig. 8). Because of the relative rotation between two adjacent blade rows, wake skew in upstream row introduces periodic variations in incidence and flow angle. The blade installation angle should be adjusted in the design process to utilize the wake skew phenomenon.

The driving force of the rotor wake skewing is the static pressure difference between pressure side and suction side of the rotor wake. Figure 10 shows the static pressure difference fluctuation over the time at 20% span position, where the static pressure difference Δp is computed as

$$\Delta p = p(\mathrm{PS}) - p(\mathrm{SS}) \tag{3}$$

where p(PS) and p(SS) are the static pressures at the pressure side and suction side of the rotor wake, respectively.

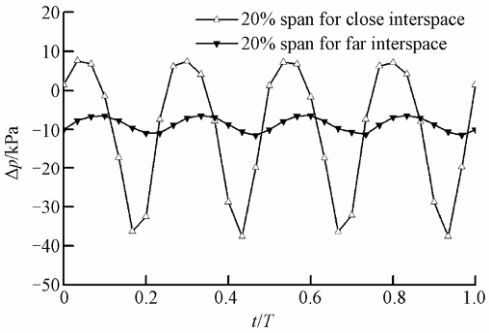

Fig.10 Static pressure difference between pressure side and suction side of the rotor wake, 20% span.

The results exhibit a similar trend for all the test models in Fig. 10, but the amplitude of the static pressure difference fluctuation induced by potential field of stator reduces as the axial interspace increases. It is well known that vector sum of momentum acted on the rotor wake will decide the rotor wake location in the relative phase. A new parameter T_r is defined to quantify the rotor wake skewing. It is computed as

$$T_\mathrm{r} = \int_0^1 f(t/T)\mathrm{d}(t/T) \tag{4}$$

where $f(t/T)$ is the static pressure difference between pressure side and suction side of rotor wake.

When the T_r value is above zero, it means that the vector sum of momentum drives the rotor wake flow to suction side of blade; while the vector sum of momentum shifts rotor wake to the pressure side of the blade as T_r is below zero; the vector sum of momentum is equal to zero when T_r=0. The vector sum of momentum will be larger for bigger absolute value of T_r. $T_{\mathrm{r,\ close\ interspace}}$ value corresponding to the curve line for close interspace is −10 359.35 by calculation, while the $T_{\mathrm{r,far\ interspace}}$ value corresponding to another line is −8 585.74. They are all below zero for both close and far interspace models, which means that the rotor wake is driven towards the pressure side of blade. In addition, because $|T_{\mathrm{r,\ close\ interspace}}|>|T_{\mathrm{r,\ far\ interspace}}|$, we can conclude that the skewing value of rotor wake corresponding to close interspace model is larger than that for far interspace model. Different positions of rotor wake in Fig. 8 provide the evidence to illustrate that the above analysis is true.

3.4. Flow angle variability at rotor exit

Not only the rotor wake characteristic (wake oscillation and skewing) is influenced by downstream stator but also the absolute flow angle can be changed by interaction with downstream stator. As shown in Fig. 11, the axial velocity variability in the relative frame corresponds to a change in flow angle at the stator inlet in the absolute reference frame. Moreover, because of rotor wake velocity deficit, the absolute flow angle α is larger in wake region than that in other regions.

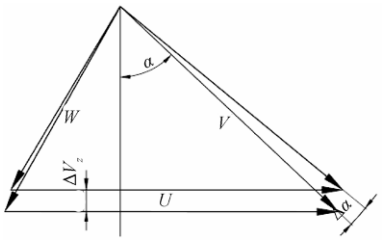

Fig. 11 Velocity triangle for compressor rotor exit.

Figure 12 compares absolute flow angle fluctuation at rotor exit for both close and far interspace models in absolute phase. On the one hand, the absolute value is increased obviously for each time step in the case of the close interspace model than that in the case of the far interspace model. On the other hand, the amplitude of the revolution waveform appears larger in close interspace model than that in far interspace model. This indicates that interaction strength by downstream stator blockage is weakened through increasing the axial distance between rotor and stator rows, which leads to

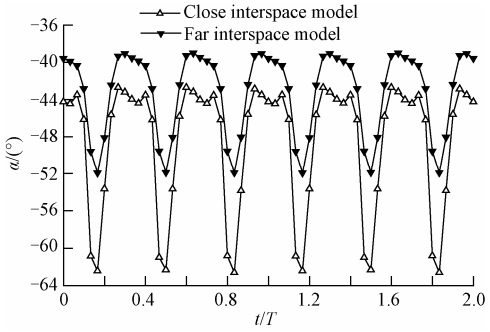

Fig. 12 Absolute flow angle fluctuation at rotor exit (in absolute phase).

absolute flow angle variability and has an effect on the vane life, finally.

4. Conclusions

1) The amplitude of rotor wake oscillation is associated with the axial distance between rotor and stator rows. Obvious oscillation phenomenon appears in the close interspace model, while the phenomenon disappears in the far interspace model. Moreover, the amplitude decreases along spanwise direction, because of the increased axial distance along radial direction.

2) The tangential static pressure gradient is induced by potential field of downstream stator, which mainly contributes to the rotor wake oscillation. The positive tangential pressure gradient drives the rotor wake to oscillate towards the pressure side of blade, and the negative pressure gradient drives the wake to rightabout.

3) The rotor wake's position skewing is connected with blade-row interspace. The rotor wake's position locates at the range from 0.5 to 0.55 pitches for the close interspace model, while it shifts with the distance of about 5%-10% amplitude of the pitch towards the suction side in far interspace model. The vector sum of momentum acted on wake skewing decides the orientation and amplitude of wake skewing.

4) The flow angle fluctuation is influenced by geometry blockage strength of downstream vane at rotor exit. The axial velocity is changed by downstream stator leading edge, which leads to different amplitudes of absolute flow angle fluctuation and varied absolute values of instantaneous values for two models. They can be modulated by changing blade-row distance.

Reference

[1] Oro J M F, Diaz K M A, Morros C S, et al. Analysis of the deterministic unsteady flow in a low-speed axial fan with inlet guide vanes. Journal of Fluids Engineering 2008; 130(3): 031101.1-031101.12.

[2] Key N L, Lawless P B, Fleeter S. Rotor wake variability in a multistage compressor. Journal of Propulsion and Power 2010; 26(2): 344-352.

[3] Strazisar A J. Investigation of flow phenomenon in a transonic fan rotor using laser anemometry. NASA-TM-83555, 1984.

[4] Albert J S, Fleeter S. Rotor blade-to-blade wake variability and effect on downstream vane response. Journal of Propulsion and Power 2002; 18(2): 456-464.

[5] Mailach R, Vogeler K. Aerodynamic blade row interactions in an axial compressor-part I: unsteady boundary layer development. ASME Journal of Turbomachinery 2004; 126(1): 35-44.

[6] Estevadeordal J, Gorrell S, Copenhaver W W. PIV study of wake-rotor interactions in a transonic compressor at various operating conditions. Journal of Propulsion and Power 2007; 23(1): 235-242.

[7] Mao M M, Song Y P, Wang Z Q. Numerical research on influence of rotor-stator interactions in transonic compressor. Journal of Aerospace Power 2007; 22(9): 1468-1474. [in Chinese]

[8] Li S B, Su J X, Feng G T, et al. Study of performance and profile pressure distribution of transonic compressor under rotor-stator interaction condition. Journal of Aerospace Power 2007; 22(7): 1153-1160. [in Chinese]

[9] Li X S, Feng F, Gu C W. Detached eddy simulation for the stator-rotor interaction. Journal of Engineering Thermophysics 2009; 30(6): 953-956. [in Chinese]

[10] Miller R J, Moss R M, Ainsworth R W, et al. Wake, shock, and potential field interactions in a 1.5 stage turbine-part I: vane-rotor and rotor-vane interaction. ASME Journal of Turbomachinery 2003; 125(1): 33-39.

[11] Gorrell S E，Car D，Puterbaugh S L. An investigation of wake-shock interactions in a transonic compressor with digital particle image velocimetry and time-accurate computational fluid dynamics. ASME Journal of Turbomachinery 2006; 128(4): 616-626.

[12] Li W, Sun Y, Ren Y X, et al. The influence of rotor-stator spacing on the loss in one-stage transonic compressor. ASME Paper, GT-2009-59762, 2009.

[13] Yan Z, Ji L C, Chen J, et al. Investigation about the effects of axial gaps on clocking effects. Journal of Engineering Thermophysics 2004; 25(2): 220-222. [in Chinese]

[14] Reid L, Mooer R D. Performance of single-stage axial-flow transonic compressor with rotor and stator aspect ratios of 1.19 and 1.26, respectively, and with design pressure ration of 1.82. NASA-TP-1338, 1978.

[15] Chima R V. SWIFT code assessment for two similar transonic compressors. AIAA-2009-1058, 2009.

[16] Wo A M, Chung M H, Hsu S T. Gust response decomposition in a stator/rotor axial compressor with varying axial gap. Journal of Propulsion and Power 1997; 13(2): 178-185.

[17] Lu H W, Chen F, Wan J L, et al. Flow field improvement by bowed stator stages in a compressor with different axial gaps under near stall condition. Chinese Journal of Aeronautics 2008; 21 (3): 215-222.

[18] Zhao B, Yang C, Zhang J Z, et al. Stator wake variability in a combined compressor. Journal of Aerospace Power 2012; 27(2): 410-418. [in Chinese]

Biographies:

ZHAO Ben received M.S. degree in 2009 from China University of Petroleum. Currently he is a Ph.D. candidate in Beijing Institute of Technology. His research interest is the unsteady flow in turbomachinery.
E-mail: Zhaoben27@163.com

YANG Ce is a professor and Ph.D. supervisor at School of Mechanical Engineering, Beijing Institute of Technology, Beijing, China. He received the Ph.D. degree from the Tsinghua University in 1998. His current research interest is the unsteady flow in turbomachinery.
E-mail: yangce@bit.edu.cn